Mathematical modeling and simulation of perlite grain expansion in a vertical electrical furnace

5th International Conference from Scientific Computing to Computational Engineering
5th IC-SCCE
Athens, 4-7 July, 2012

MATHEMATICAL MODELING AND SIMULATION OF PERLITE GRAIN EXPANSION IN A VERTICAL ELECTRICAL FURNACE

Panagiotis M. Angelopoulos[1*], Dimitrios I. Gerogiorgis[2], and Ioannis Paspaliaris[3]

Laboratory of Metallurgy
School of Mining and Metallurgical Engineering
National Technical University of Athens
Athens, GR-15780, Greece

e-mail: [1] pangelopoulos@metal.ntua.gr, [2] dgerogiorgis@metal.ntua.gr, [3] paspali@metal.ntua.gr

Keywords: Perlite expansion, vertical electrical furnace, dynamic modeling, process design, process simulation.

Abstract. *Expanded perlite has outstanding thermal and acoustic insulating properties and is widely used in the manufacturing and construction industries. The conventional perlite expansion method suffers disadvantages which affect the quality of expanded perlite products, thus limiting their performance and range of applications. A new perlite expansion process has been designed and a vertical electrical furnace for perlite expansion has been constructed in our laboratory to overcome these drawbacks: the new design enables precise control of experimental conditions, so as to prescribe the temperature profile and residence time in the heating chamber. Expanded perlite can thus be produced with various quality specifications for a range of different applications. A mathematical model for perlite grain expansion has been developed, aimed at the detailed investigation and optimization of perlite expansion in the new furnace. The dynamic model consists of ordinary differential equations for both air and particle heat and momentum balances, probing the air temperature distribution as well as the particle velocity, temperature and size along its trajectory in the heating chamber. The effect of raw material physical properties as well as operational parameters on product quality is investigated and discussed.*

1 INTRODUCTION

Perlite is a natural occurring volcanic siliceous rock which consists mainly of amorphous silica (70-76 % wt.) but also contains smaller quantities of numerous other metal oxides (Al_2O_3, K_2O, Na_2O, Fe_2O_3, CaO, MgO). Perlite can be expanded from 4 to 20 times its original volume when heated at a temperature close to its softening point (700-1260 °C), due to the presence of 2-6% chemically bound water within its microstructure [1]. Conventional perlite expansion is usually accomplished by feeding ground, pre-sized perlite ore into a vertical furnace heated by a direct gas flame at its bottom end, thus directing forced air flow upwardly: ore particles are typically introduced into the hottest expansion chamber region, near the flame, at a temperature of 1450 °C [2]. During expansion, perlite acquires outstanding physical properties (e.g. low density, thermal and acoustic insulation) which render it suitable for numerous applications in the construction and manufacturing industries. The currently prevalent perlite expansion process is virtually the only globally reliable production method: although it has been in continuous use for more than 50 years, it remains a largely empirical industrial process, despite the rapid increase and proliferation of expanded perlite uses and applications over the past few decades. Its main technical problems include the increased heat losses due to the off-gas stream, leading to high energy consumption, but also the violent and poorly controlled heating of perlite which results in an expanded material with unfavourable mechanical properties, which adversely affect quality and limit the range of its applications.

To overcome these drawbacks, a novel perlite expansion process has been designed and a new pilot-scale production unit has been constructed, based on the concept of a vertical, electrically heated expansion furnace. The new vertical electrical furnace has been designed for maximizing experimental flexibility, in order to facilitate the adjustment of operating conditions versus raw material but also final product quality specifications. The new perlite expansion method allows the milder, gradual heating of perlite grains, as well as the variation of perlite grain residence time in the heating chamber. Experimental perlite expansion campaigns conducted on this pilot-scale production unit indicate a remarkable improvement as well as a definite operating cost reduction in expanded perlite properties compared with conventional processing. Hence, the multi-parametric mathematical investigation of the process system thermal behavior and the identification of the effect of all crucial operational parameters on perlite expansion dynamics is an endeavor of evident importance which must guide the eventual optimization of the entire pilot-scale experimental facility and every subsequent production-scale process. Investigating the effect of key operational parameters on product quality yields profound process understanding.

2 THE VERTICAL ELECTRICAL FURNACE CONFIGURATION AND OPERATION

2.1 Vertical electrical perlite expansion furnace

The vertical electrical perlite expansion furnace consists of the air preheater and flow control system, the perlite feeding system, the heating chamber and the furnace temperature control system (Figure 1). Atmospheric air is introduced into the system by an air compressor and the volumetric flow rate is measured and controlled by a dedicated system of flowmeters and valves. The air is injected at the top of the furnace through six 0.009 m-diameter holes located symmetrically around the perlite inlet hole and at a distance of 0.044 m from the center. Air can be heated by a preheater which has a heat capacity of 2 kW and can raise temperature to up to 450 °C. The desirable perlite feeding rate is achieved by a rotary air-lock feeder, through a 0.08 m diameter central hole. The rotary air-lock feeder prevents hot air upward drafts but also the escape of perlite particles from the furnace.

The cylindrical heating chamber is 3 m long and 0.134 m wide, and is made of Kanthal APM FeCrAl alloy. The chamber is heated by 6 pairs of electrical resistances located along the tube, defining six heating zones. Each pair consists of two semicylindrical Kanthal resistances, located against each other around the chamber and at a distance of about 3 cm out of it, providing a total heating capacity of 24 kW to the expansion process. The chamber and resistances are encased in a cylindrical alunimosilicate insulation case of 0.165 cm thickness. Temperature measurements within each thermal zone are obtained via a ceramic sheathed K-type thermocouple (NiCr/NiAl) placed at each zone center; air inlet temperature is measured by a thermocouple located before the furnace head. Preheater as well as heating zone temperatures can all be individually controlled by the operator.

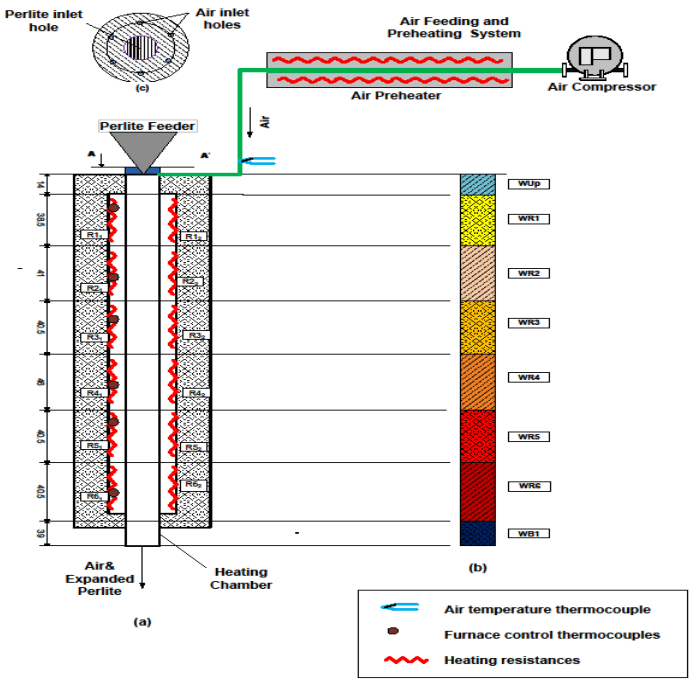

Figure 1. Schematic of the prototypic experimental installation constructed at NTUA for perlite expansion, illustrating the vertical electrical furnace and head layout, its 6 electrical heating zones and all auxiliary systems.

2.2 Dynamic mathematical modeling assumptions

The fundamental assumptions for developing the macroscopic and microscopic parts of the mathematical model are important in order to understand the scope and accuracy of the model as well as the limits of its applicability. Air is introduced through the entire face of the cylindric chamber, without any pressure drop (P = 1 atm): its temperature along the heating chamber has no radial variation, and the entire chamber wall surface is smooth. Air temperature and velocity distributions are studied via one-dimensional models, as radial air velocity is zero. The effect of air components which are not transparent to thermal radiation (CO_2, H_2O) is negligible and does not affect air heating. Each perlite grain is considered perfectly spherical throughout the expansion process, and has a uniform temperature which varies during expansion only because of heating and evaporation phenomena. Perlite shell melt, thermal conductivity and specific heat capacity are considered constant throughout expansion. Diffusion or mass transfer across the bubble-shell and the shell-environment interface have not been considered. The entire amount of the effective water content within the perlite grain is concentrated at the steam bubble nucleus throughout the expansion process. Steam obeys the ideal gas law in the entire process. The enthalpy of water evaporation inside grains is explicitly considered, but mechanical work for bubble expansion is negligible.

3 AIR AND PERLITE MELT PROPERTIES

3.1 Air thermophysical properties

Air can be injected into the heating chamber at a temperature of 25 °C and heated up to 1200 °C: property variations are expected to be dramatic, so incorrect estimates induce significant error in energy balance models. The estimation of a mean air temperature in the heating chamber is used for air transport property calculations:

$$T_{mean} = \frac{T_{air,in} + T_w}{2} \tag{1}$$

Here, T_{mean} is the mean air temperature, while $T_{air,in}$ and T_w are the air temperature at the inlet of the furnace and the heating chamber wall temperature (both in K), respectively. The air density variation affects the volumetric air flow rate along the vertical heating chamber, inducing an increase of superficial air velocity; it also affects the buoyancy and drag forces on perlite grains and the convective heat transfer rate from the air to the particle. Air density variation along the vertical heating chamber is calculated by the ideal gas law constitutive equation:

$$\rho_{air} = \frac{P}{R_g T_{air}} \tag{2}$$

Here, ρ_{air} is the air density (kg·m^{-3}), R_g is the ideal gas law constant and pressure is taken constant (P = 1 atm). The model assumes constant air dynamic viscosity (μ_{air}), heat capacity (k_{air}), thermal conductivity (C_{Pair}) and Prandtl number (Pr_{air}) at mean temperature. Air thermophysical properties are calculated by the next equations:

$$\mu_{air} = \mu_{air,ref}\left(\frac{T_{air,mean}}{T_{air,ref}}\right)^{n_{ref}} \tag{3}$$

Parameter values for air viscosity calculation are: $\mu_{air,ref}$ = 1.72·10^{-5} Pa·s, $T_{air,ref}$ = 273 K, n_{ref} = 0.7, respectively.

$$C_{p,air} = \alpha_{C_p,1} T_{air,mean}^{\ 3} + \alpha_{C_p,2} T_{air,mean}^{\ 2} + \alpha_{C_p,3} T_{air,mean} + \alpha_{C_p,4} \tag{4}$$

Coefficient values for $\alpha_{Cp,1}, \alpha_{Cp,2}, \alpha_{Cp,3}, \alpha_{Cp,4}$ are: -8.01440·10^{-8}, 2.10788·10^{-4}, 2.06329·10^{-2}, 9.83672·10^{2}, respectively.

$$k_{air} = \alpha_{k,1} T_{air,mean}^{\ 3} + \alpha_{k,2} T_{air,mean}^{\ 2} + \alpha_{k,3} T_{air,mean} + \alpha_{k,4} \tag{5}$$

Coefficient values for $\alpha_{k,1}$, $\alpha_{k,2}$, $\alpha_{k,3}$, $\alpha_{k,4}$ are: -1.5207·10^{-11}, -4.8574·10^{-8}, 1.0184·10^{-4}, -3.9333·10^{4}, respectively.

3.2 Perlite melt thermophysical properties

In our research we investigated perlite ore particles obtained from the Trachylas mine (Milos island, Greece). The perlite ore considered in this modeling study consists of amorpous silica (73% wt. SiO_2), aluminium oxide (12.7% Al_2O_3), other metal oxide amounts (K_2O, Na_2O, Fe_2O_3, CaO) and 3.32 % LOI (Lost On Ignition) matter. Water plays the most important role during the entire expansion process, not only by expanding the grain during evaporation but also by reducing the viscosity of the softened grain shell; the amount of perlite water which is available and responsible for its potential to expand on heating has been studied by previous publications [3][4]. Based on LOI tests, we conclude that a water portion remains in the expanded grain without participating in expansion: this is the *residual water* (40%) which is only considered in perlitic melt thermophysical property calculation, while the remaining *effective water* (60%) drives steam bubble growth and perlite grain expansion. Perlite melt density is assumed constant (ρ_m = 2300 kg·m^{-3}) in the entire grain temperature range; Zahringer *et al.* used a mean value of 2350 kg·m^{-3}, while Proussevitch *et al.* used a rhyolitic melt density of 2200 kg·m^{-3} [5][6]. Our raw perlite ore density measurement (2290 kg·m^{-3}) agrees with melt density values reported in the literature.

Perlite expansion evolution is affected by molten grain shell viscosity, which varies significantly during the process and is a strong function of temperature: in a relevant publication, Giordano *et al.* studied compositional and temperature effects on magmatic liquid viscosity, developing a multi-parametric algebraic model which is used here and calculates melt viscosity as a function of both chemical composition and absolute temperature [7]. The temperature dependence of viscosity is accounted for by the Vogel-Fulcher-Tammann (VFT) equation [8][9], with J, X and Y (pre-exponential factor, pseudo-activation energy and VFT temperature, respectively) all given:

$$\log\mu = J + \frac{X}{T_m - Y} \tag{6}$$

The surface tension exerted on the shell-bubble interface is crucial, since it counteracts bubble expansion. The temperature dependence of perlitic melt surface tension (σ) with respect to temperature can be approximated by a published linear correlation for obsidian (0.5% wt. H_2O), valid in the 1000-1400 ^{o}C range [5]:

$$\sigma = 0.09317 + 1.971\cdot10^{-4}\,T_m \tag{7}$$

4 THE MATHEMATICAL MODEL

The dynamic mathematical model which we have developed concentrates on the momentum and energy balance description of single-grain expansion in the vertical electrical furnace, at a microscopic and a macroscopic level. Microscopic mathematical analysis here refers to the investigation of internal particle temperature and steam bubble pressure evolution, as the interplay and rates of both these phenomena governs perlite grain expansion. Macroscopic mathematical analysis refers to particle motion (force balance) and air temperature distribution. These transport phenomena are analyzed via a nonlinear system of algebraic and ordinary differential equations.

4.1 Perlite particle motion along the vertical heating chamber

The forces exerted on the falling particle are the gravitational force (F_G) which accelerates the particle, the drag force (F_D) and the buoyancy force (F_B) which decelerate the perlite grain vertical fall by opposing its motion:

$$F_G = m_p g \qquad (8) \qquad F_D = \frac{1}{2}\rho_{air} C_D A_{proj} \left(U_{air} - U_p\right)^2 \qquad (9) \qquad F_B = \rho_{air} g V_p \qquad (10)$$

The momentum balance on the falling perlite particle follows Newton's second law of mechanics: considering all forces exerted on a grain, the particle velocity evolution is calculated by an ordinary differential equation[10]:

$$\sum F = m_p \frac{dU_p}{dt} \Rightarrow \frac{dU_p}{dt} = \frac{\rho_p - \rho_{air}}{\rho_p} g - \frac{3}{4} \frac{\rho_{air} C_D \left(U_{air} - U_p\right)^2}{d_p \rho_p} \qquad (11)$$

The drag force coefficient (C_D) is calculated via a correlation based on the particle Reynolds number (Re_p) [10] :

$$C_D = \frac{K_1}{\mathrm{Re}_p} + \frac{K_2}{\mathrm{Re}_p^2} + K_3 \qquad (12)$$

The particle Reynolds number (Re_p) is calculated based on the relative velocity by the following equation [11]:

$$\mathrm{Re}_p = \frac{\rho_{air} d_p \left|U_p - U_{air}\right|}{\mu_{air}} \qquad (13)$$

The volumetric air flow rate due to the increase of air temperature and the decrease of air density along the grain trajectory in the heating chamber is taken into account toward air velocity calculation by the following equation:

$$U_{air} = \frac{\dot{Q}_{air,in} T_{air}}{A_{tube} T_{air,in}} \qquad (14)$$

4.2 Air heat balance in the vertical heating chamber

The problem of air temperature calculation in the heating chamber can be considered and solved as follows: air is injected into a vertical tube and flows at mean velocity, within heated furnace walls of constant temperature. Thermal energy is transferred to the fluid (air) by convection, thereby causing an increase in the air temperature. Air temperature calculation is based on an adiabatic energy balance, with the initial condition T_{air} (t = 0) = $T_{air, in}$.

$$\frac{dT_{air}}{dt} = \left(\frac{\pi d h_{mean}}{\dot{m} C_{p_{air,mean}}} \right) \left(T_w - T_{air}\right) \qquad (15)$$

The mean convective heat transfer coefficient (h_{mean}) therein is calculated by the following algebraic equation:

$$h_{mean} = \frac{k_{air} Nu_{mean}}{d} \qquad (16)$$

The mean Nusselt number along the heating chamber is calculated by Hausen's equation, which explicitly includes the effect of the thermal entry length, within which the heat transfer coefficient is not yet constant [12]:

$$Nu_{mean} = Nu_\infty + \left[\frac{0.104 \left(\left(\frac{d}{L} \right) \mathrm{Re}_t \, \mathrm{Pr}_{air} \right)}{1 + 0.016 \left(\left(\frac{d}{L} \right) \mathrm{Re}_t \, \mathrm{Pr}_{air} \right)^{0.8}} \right] \left(\frac{\mu_{air}}{\mu_w} \right) \qquad (17)$$

4.3 Perlite grain energy balance in the vertical heating chamber

The falling perlite grain is assumed to have a uniformly varying temperature, as internal gradients are negligible. The validity of this assumption is confirmed by a Biot number calculation for a compact unexpanded particle: for the thermophysical properties and conditions considered, one can numerically confirm that its value (*Bi*) does not exceed *Bi* = 0.047, even in the most unfavorable case of maximum resistance to conductive heating. As the maximum Biot number is much lower than the limit value of Bi_c = 0.1 (a case for which literature indicates that total radial temperature variation cannot exceed 5%), the uniform temperature assumption is valid.

The solid particle absorbs energy by radiation and convection: both contribute to heating and expansion and they are equally important heat transfer mechanisms in order to understand furnace as well as process efficiency. The grain temperature evolution due to radiative heating is calculated on the basis of the Stefan-Maxwell law, thus accounting for the thermal energy emitted by the furnace walls and absorbed by the moving perlite grain. Furthermore, the solid particle exchanges thermal energy with air by convective heating: this is an interesting phenomenon, as one can in fact numerically identify a sign reversal along the perlite grain trajectory: initially the cold particles are heated by the upward air current, but they are warmer than air as they approach the exit. Consequently, perlite grain temperature evolution is governed by the combination of radiative and convective heat transfer mechanisms and the dynamic heat balance is given by the following ordinary differential equation:

$$\frac{dT_p}{dt} = \varepsilon_w \cdot \frac{A_s s\left(T_w^4 - T_p^4\right)}{\rho_p V_p C_{p_p}} + \frac{A_s h_c \left(T_{air} - T_p\right)}{\rho_p V_p C_{p_p}} - \Delta H_{evap}\left(\frac{P_b}{R_g T_p}\right)\left(\frac{4\pi R_b^3}{3}\right) \tag{18}$$

Here, ε_w is the furnace wall emissivity (estimated at ε_w = 0.7 by construction) [13], A_s is the perlite particle surface area, *s* is the Stefan-Boltzmann constant and ΔH_{evap} is the molar enthalpy of water evaporation (40.68 kJ·mol^{-1}).

4.4 Steam bubble growth within the perlite grain

In the present mathematical modeling study, perlite expansion is approximated by a detailed single-grain model. The model particle consists of a spherical steam nucleus and a solid shell surrounding the steam bubble: steam is treated as an ideal gas, with no mass transfer across the steam-shell or the shell-environment interface permitted. During particle heating, the perlite grain temperature increase has a dual effect: firsly, steam enthalpy increases, thereby increasing the pressure exerted on the bubble-shell interface; concurrently, molten shell viscosity and cohesion decrease, thus facilitating bubble expansion and increasing steam bubble radius and perlite grain size.

The pressure factors acting on the bubble-shell interface are the surface tension (σ), the steam pressure (P_b), and the ambient pressure (P_a): steam pressure acts towards expanding the bubble, while both surface tension and ambient pressure act against steam bubble growth. The steam bubble only contains the entire effective water amount, since the residual water amount is uniformly dispersed in the molten shell without affecting expansion. The initial steam bubble radius ($R_{b,i}$) can be calculated by means of mass by the following algebraic equation:

$$R_{b,i} = \sqrt[3]{R_{p,i}^3 - \frac{3}{4\pi}\frac{m_m}{\rho_m}} \tag{19}$$

The molten shell mass (m_m) is calculated using the grain water mass fraction (w_{H2O}) by the following equation:

$$m_m = \left(1 - w_{H_2O}\right) m_p \tag{20}$$

The steam in the core of the grain is treated as ideal gas: its instantaneous pressure is calculated by considering the bubble radius evolution in the bubble volume term and implementing the ideal gas law constitutive equation:

$$P_b(t) = \frac{3NR_gT_p}{4\pi R_b^3(t)} \tag{21}$$

The Navier-Stokes equation for spherical creeping flow is combined with the melt radial velocity equation and the bubble surface stress balance, to yield an ordinary differential equation for bubble radius evolution [14][15][16]:

$$\frac{dR_b}{dt} = \frac{R_b}{4\mu_m}\left(P_b(t) - P_a - \frac{2\sigma}{R_b}\right) \tag{22}$$

The required initial condition is the miniscule steam bubble radius assumed at particle injection: $R_b(t = 0) = R_{b,i}$.

5 RESULTS AND DISCUSSION

A computer model has been developed so as to streamline the systematic numerical investigation of the process. The dynamic operation of the novel furnace is modeled within the Berkeley Madonna® ODE modeling platform (version 8.3.18), using a dual-core Intel Pentium T3200 (2 GHz) with 3 GB of RAM in Windows Vista (32-bit). The nonlinear system of algebraic and ordinary differential equations is solved via a 4th-order Runge-Kutta numerical integration method, using solution and reporting timesteps of $\Delta t_s = 0.01$ s and $\Delta t_r = 0.05$ s, respectively.

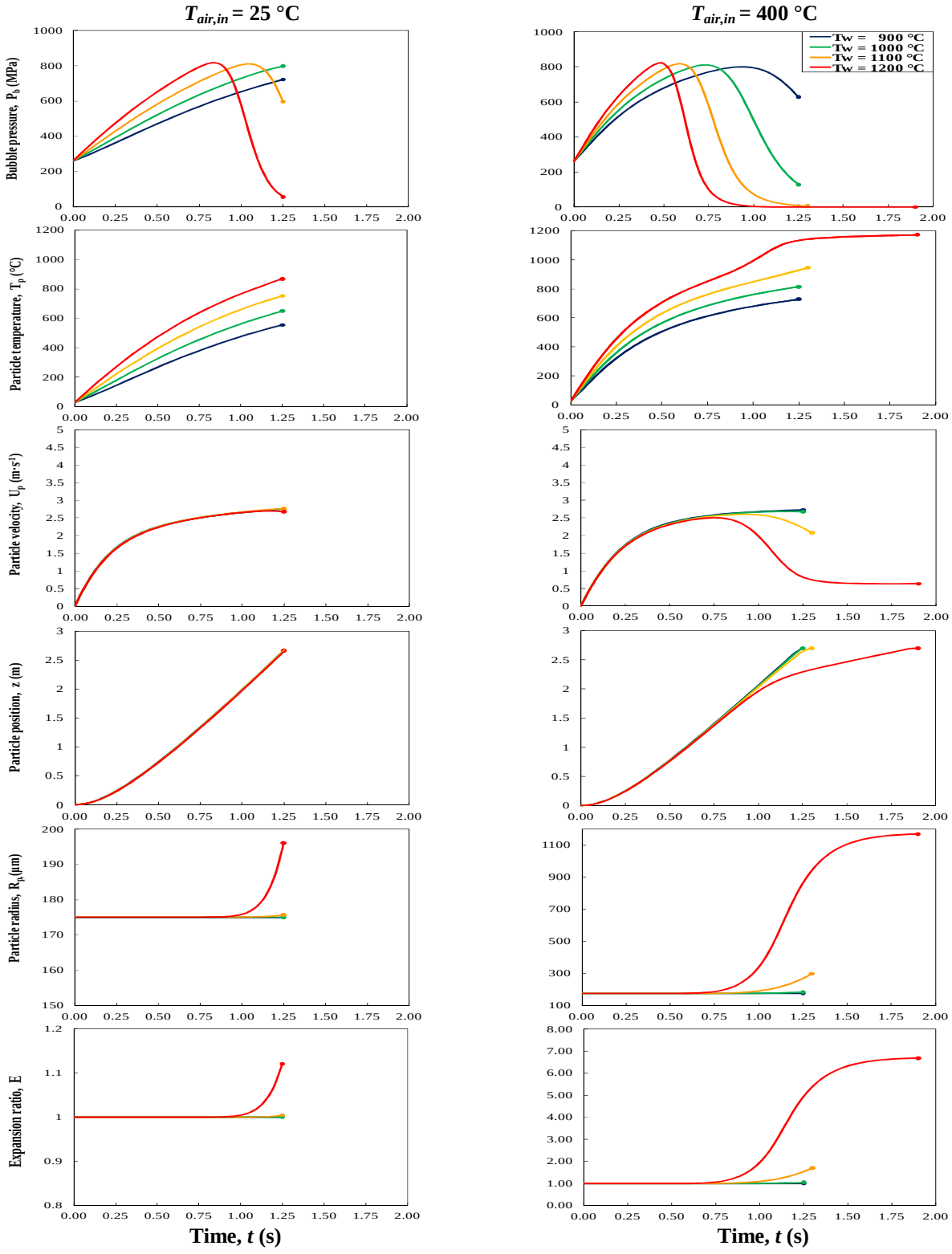

Figure 2. Temporal evolution of particle state variables as a function of heating chamber wall temperature, for the two air feed temperature extremes. Constant parameters: $Q_{air,\,in}$ = 50 L·m^{-1}, D_{pi} = 350 μm, $w_{H2O,eff}$ = 2.00 %.

Figure 2 presents all perlite particle state variables (key model outputs) for various furnace wall temperatures. Particle pressure increases due to the increase of grain temperature: a relief is observed at 600 °C, when shell viscosity and cohesion decrease and bubble radius starts expanding. Particles decelerate rapidly at expansion onset, due to the strong impact of particle radius on drag and buoyancy forces. Air preheating is paramount for effective particle heating: feeding atmospheric air at ambient temperature hinders expansion, often completely.

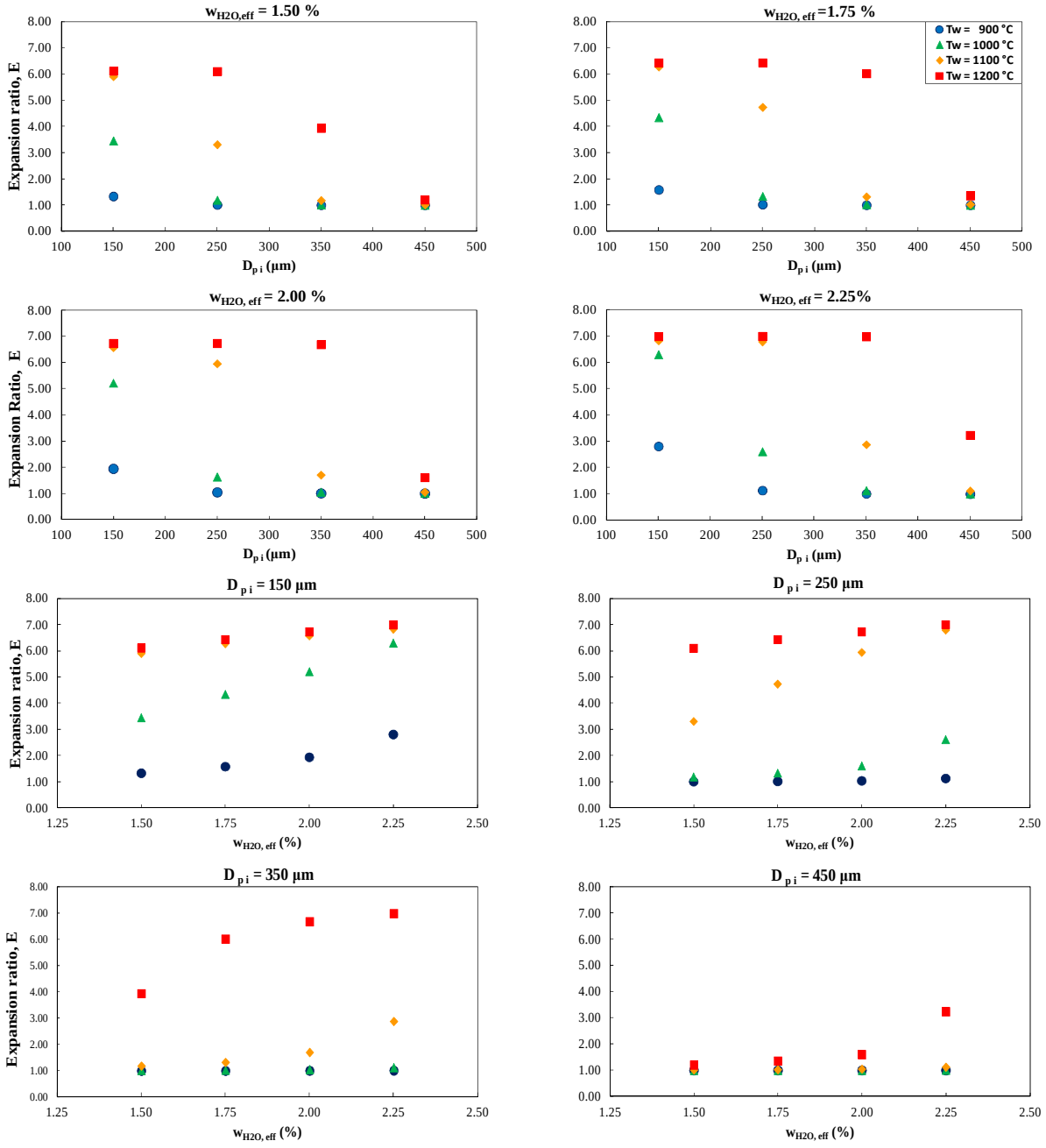

Figure 3. Final perlite particle expansion ratios achieved as a function of heating chamber wall temperature, for the entire grain size and effective water content ranges. Air feed parameters: $Q_{air,\ in}$ = 50 L·min^{-1}, $T_{air,in}$ = 400 °C.

Figure 3 presents the effect of feed physical properties on the final particle expansion ratio ($E = R_{p,\ final} / R_{p,i}$). Effective water content is critical for expansion evolution as it increases bubble pressure and decreases molten shell viscosity: hence, the higher the initial effective water content, the more efficiently perlite grains expand. The upper expansion ratio limit approximates E_{max} = 7, thus the particle diameter increases up to seven times. The expansion ratio itself is independent of effective water content and initial radius. However, initial size is critical for expansion: although finer grains expand even at T_w = 900 °C, but larger grains require T_w > 1100 °C. Heating and expansion efficiency increases for decreasing size, if the minimum residence time condition is met.

6 CONCLUSIONS

A mathematical model has been developed for perlite grain expansion within a novel vertical electrical furnace. This dynamic model consists of ordinary differential equations for both air and particle heat and momentum balances, as well as nonlinear algebraic equations for air and perlite melt thermophysical properties, probing air temperature distribution as well as particle velocity, temperature and size along its trajectory in the chamber. The model computes particle state variables evolution as well as air temperature distribution in the furnace, allowing the detailed investigation of a new perlite expansion method towards its cost-effective optimization. Process operating parameter (air and furnace wall temperature) and raw material physical property variations have been considered as dynamic model inputs, in order to probe their relative effect on expansion efficiency. The major conclusion of this modeling study is that the novel vertical electrical furnace design can successfully accomplish perlite expansion up to final product quality standards, within an acceptably wide operating regime. Preheated air injection is clearly crucial towards adequate perlite heating and expansion, because cold air usage results either in no expansion or in unacceptable product quality; air flowrate requires further investigation. Raw material physical properties also affect perlite expansion efficiency dramatically, indicating that vertical electrical furnace tuning has paramount importance in order to ensure expansion for variable feed grade quality. An important distinction must be made between residual and effective water contain within each perlite grain. Higher particle water contents lead to higher expansion ratios as long as preheated air is injected in the chamber, and the effect of furnace wall temperature increases spectacularly in the temperature range of 1100-1200 °C. Consequently, a detailed numerical and experimental investigation therein is required for process optimization. The short residence time computed for large perlite grains in the furnace indicates that heating rate may be inadequate, so expansion may not commence due to the unfavorable interplay of gravity, shape and air injection. Consequently, air feed flow rate dynamic adjustment is a very likely requirement for raw perlite grade variation.

ACKNOWLEDGEMENTS

This work has been financed by the European Union Seventh Framework Programme (project CP-IP 228697-2, Efficient exploitation of EU perlite resources for the development of a new generation of innovative and high added value micro-perlite based materials for the chemical, construction and manufacturing industry, EXPERL). Mr. P. Angelopoulos would like to also acknowledge the financial support of the Greek Scholarship Foundation.

REFERENCES

[1] Chatterjee, K.K. (2008), *Uses of Industrial Minerals, Rocks and Freshwater*. Nova Science Publishers, New York, USA.

[2] Papanastassiou, D.J. (1979), "Perlite expansion in a vertical furnace – A simplified theoretical analysis". *Proceedings of the Perlite Institute Annual Meeting*, Dubrovnik, Yugoslavia, pp. 67-71.

[3] King, E.G., Todd, S.S., Kelley, K.K. (1948), "*Perlite thermal data and energy required for expansion*" United States Bureau of Mines.

[4] Shackley, D. (1988), *Characterization and Expansion of Perlite*, PhD Thesis, Univ. of Nottingham, UK.

[5] Zahringer, K., Martin, J.-P., Petit, J.P. (2001), "Numerical simulation of bubble growth in expanding perlite", J. Mater. Sci., Vol. 36, pp. 2691-2705.

[6] Proussevitch, A.A, Sahagian, D.L. (1998), "Dynamics and energetics of bubble growth in magmas: Analytical formulation and numerical modeling", J. Geophys. Res., Vol. 103, pp. 18223-18252.

[7] Giordano, D., Russell, J.K., Dingwell, D.B. (2008), "Viscosity of magmatic liquids: A model", Earth Planet Sc. Lett., Vol. 271, pp. 123-134.

[8] Vogel, D.H. (1921), "Temperaturabhängigkeitsgesetz der Viskosität von Flüssigkeiten", Z. Phys. Chem., Vol. 22, pp. 645-646.

[9] Fulcher, G.S., (1925). "Analysis of recent measurements of the viscosity of glasses", J. Am. Ceram. Soc., Vol. 8, pp. 339-355.

[10] Morsi, S.A., Alexander, A.J. (1972), "An investigation of particle trajectories in two-phase flow systems", J. Fluid Mech., Vol. 55, pp. 193-208.

[11] Liang, S.F., Zhu, C. (1998), *Principles of Gas-Solid Flows*. Cambridge University Press, Cambridge, UK.

[12] Hausen, H. (1943), *Darstellung des Warmenberganges in Rohren durch verallgemeinerte Potenzbeziehungen*, VDI Z Beihefte Verfahrenstechnik, Germany.

[13] Kanthal: www.kanthal.com/en/products/material-datasheets/tube/kanthal-apm/ (Accessed: 30/5/2012).

[14] Patel, R.D. (1980), "Bubble growth in a viscous Newtonian liquid". Chem. Eng. Prog., Vol. 35, pp. 2352-2356.

[15] Pai, V., Favelukis, M. (2002), "Dynamics of spherical bubble growth", J. Cell. Plas., Vol. 38, pp. 403-419.

[16] Elshereef, R., Vlachopoulos, J., Elkamel, A. (2010), "Comparison and analysis of bubble growth and foam formation models". Engrg. Comput., Vol. 27, pp. 387-408.